Heliyon 10 (2024) e37196

Contents lists available at ScienceDirect

Heliyon

journal homepage: www.cell.com/heliyon

Research article

# Phytochemical analysis, antioxidant, anticancer, and antibacterial potential of *Alpinia galanga* (L.) rhizome

Ibrahim M. Aziz [a], Akram A. Alfuraydi [a], Omer M. Almarfadi [b], Mourad A.M. Aboul-Soud [c], Abdullah K. Alshememry [d], Asma N. Alsaleh [a], Fahad N. Almajhdi [a,*]

[a] *Department of Botany and Microbiology, College of Science, King Saud University, Riyadh, 11451, Saudi Arabia*
[b] *Department of Pharmacognosy, College of Pharmacy, King Saud University, P.O. Box 2457, Riyadh, 11451, Saudi Arabia*
[c] *Department of Clinical Laboratory Sciences, College of Applied Medical Sciences, King Saud University, P.O. Box 10219, Riyadh, 11433, Saudi Arabia*
[d] *Department of Pharmaceutics, College of Pharmacy, King Saud University, Riyadh 11451, Saudi Arabia*

ARTICLE INFO

*Keywords:*
*Alpinia galanga*
Anticancer
Antimicrobial
antioxidant
Galangal
Molecular docking

ABSTRACT

*Alpinia galanga (L.)* Willd. (*A. galanga*) is extremely significant and is utilized extensively in traditional medicine throughout many nations. This study aimed to determine the chemical composition of *A. galanga* rhizome extract (AgRE) and to evaluate its antioxidant, anticancer, and antibacterial activities. The total phenolic content (TPC) and total flavonoid content (TFC) of AgRE were determined. The antioxidant activity, cytotoxic capability, and antibacterial of were assessed, as well as anti-apoptotic genes. Molecular docking (MD) was used to assess the binding affinity of the most enriched constituents in AgRE toward the active sites of nicotinamide adenine dinucleotide phosphate (NADPH) oxidase and p53 tumor suppressor protein (TP53). Gas chromatography-mass spectrometry (GC-MS) analysis demonstrated that AgRE is a rich source of turmerone. AgRE had moderate 2,2-diphenyl-1-picrylhydrazyl (DPPH) and 2,2′-azino-bis (3-ethylbenzothiazoline-6-sulfonic acid) (ABTS) radical scavenging properties, with the half-maximal inhibitory concentration ($IC_{50}$) values of 79.34 ± 1.78 and 88.94 ± 2.28 μg/ml, respectively. AgRE preferentially reduced the viability of a subset of malignant MCF-7 and HepG2 cell lines, with $IC_{50}$ of 125.35 ± 4.28 and 182.49 ± 3.19 μg/ml, respectively. AgRE exhibited considerable antimicrobial activity against all bacterial strains, with MIC values ranging from 7.81 ± 1.53 to 62.5 ± 3.28 μg/ml. The MD results revealed that ethyl-4-(2-methylpropyl)-benzene had the greatest binding energy with NADPH oxidase, with a Glide score of −6848 kcal/mol, followed by 2-methoxy-phenol (−5111 kcal/mol). Taken together, we report the interesting antioxidant, antibacterial, and anticancer properties of AgRE, which warrant further investigation. AgRE is a promising natural resource that could be used to combat complicated diseases such as cancer and bacterial infections.

* Corresponding author.
*E-mail addresses:* iaziz@ksu.edu.sa (I.M. Aziz), aalfuraydi@ksu.edu.sa (A.A. Alfuraydi), oalmarfadi@ksu.edu.sa (O.M. Almarfadi), maboulsoud@ksu.edu.sa (M.A.M. Aboul-Soud), aalshememry@ksu.edu.sa (A.K. Alshememry), asmalsaleh@ksu.edu.sa (A.N. Alsaleh), majhdi@ksu.edu.sa (F.N. Almajhdi).

https://doi.org/10.1016/j.heliyon.2024.e37196
Received 28 July 2024; Received in revised form 20 August 2024; Accepted 29 August 2024
Available online 31 August 2024

## 1. Introduction

Secondary metabolites with substantial medicinal effects are abundant in therapeutic plants [1–3]. In recent decades, several antioxidative, anticancer, anti-inflammatory, and antibacterial natural plant-derived compounds have been generated via various signaling transduction pathways [4]. Approximately 25 % of modern medicines are of plant origin, and up to 200 species are considered therapeutic plants globally [5].

*Zingiberaceae*, or the ginger family, includes *Alpinia galanga* (L.) Willd. (*A. galangal*), sometimes referred to as galangal or bigger galangal, as a perennial plant. Indonesian and other South East Asian cuisines heavily incorporate this spice. This plant is extremely significant and is utilized extensively in traditional medicine throughout many nations, particularly in India's Ayurvedic medical system. Moreover, it is a garden plant, particularly the variegated one that is primarily grown along fence lines as a foliage plant. In Asia, these rhizomes have long been utilized as spices and flavoring components because of their strong, aromatic scents and spicy taste. A well-known traditional Chinese medicine, they have been used extensively to treat gastrointestinal disorders such as dyspepsia, gastro-frigid vomiting, and stomachaches [6]. *A. galanga* is a perennial herb with beautiful blooms and lovely foliage [7]. It has thick, spreading reddish-brown rhizomes, lineolate acuminate decorative leaves, and beautiful white flowers in racemes [8]. AgRE has been widely used as a spice and food flavoring agent and in Chinese, Ayurvedic, Thai, and Unani traditional medicines to treat a variety of diseases, including stomach aches, diarrhea, diabetes, microbial infections, bronchitis, and chronic enteritis [9–12].

Secondary metabolites of *A. galanga*, including phenolic acids, flavonoids, saponins, terpenes, and essential oils, are associated with these medicinal effects [13]. The essential oils of AgRE are particularly effective as an anticancer, antioxidant, insecticidal, and anti-inflammatory agent [11,14]. The galangal rhizome extract was also found to have strong antioxidant activity, as measured by, 2, 2-diphenyl-1-picrylhydrazyl (DPPH) (77.76 %) and ABTS (8.66 mmol TE/g). Tert-butylhydroquinone, propyl gallate, butylated hydroxytoluene (BHT), and butylated hydroxyanisole (BHA) are the most used antioxidants. The DPPH and ABTS radical scavenging activities of BHA, BHT, and Trolox were around 72–96 % and 94–96 %, respectively [15].

A rapidly growing field of study examines the potential of chemicals produced by plants for preventing cancer. In addition, there is a growing body of study on these chemicals' potential anticancer properties [16,17]. One of the most well-known anticancer drugs produced from plants is paclitaxel, often known as Taxol®. This taxane dipertene cytotoxic action was discovered in extracts from *Taxus brevifolia* bark [18] A novel benzenesulfonamide incorporating a 1,2,3-triazole scaffold has shown strong antiproliferative activity and low cytotoxicity against L929, MCF-7, and Hep-3B cell lines [19].

Nowadays, most drugs used in therapeutic settings work by inhibiting or activating enzymes to produce their pharmacological effects. To ascertain the binding interactions on the active site of the Paraoxonase-I (PON1) enzyme, a prior investigation based on MD studies of several medicines, including pemetrexed disodium, irinotecan hydrochloride, dacarbazine, and azacytidine, was conducted. PON1 was shown to be substantially inhibited by these drugs, with Ki constants ranging from 8.29 $\pm$ 1.47 μM to 23.34 $\pm$ 2.71 mM [20]. However, the molecular mechanism through which extracts of AgRE have their biological effects remains elusive and incompletely understood.

Interestingly, just a few experimental investigations in the field of *A. galanga* study have provided a limited understanding of the cytotoxic and antibacterial properties of the *A. galanga* extract. The chemical composition and antibacterial activity of the crude extract and essential oils from the dried rhizome of *A.galanga* were assessed *against Salmonella typhymurium*, *Vibrio cholera*, *Bacillus subtilis*, and *Escherichia coli*, among other foodborne bacteria. The studied bacteria showed moderate growth inhibitory action when exposed to crude extracts and essential oils of galangal, with MIC values of 1000 μg/mL or more. The galangal crude extract and essential oil had MICs of 125 and 62.5 μg/mL, respectively, and *B. subtilis* was sensitive to both [21]. Moreover, *A. galanga* has shown promise in the management and decrease of sexual dysfunction associated with selective serotonin reuptake inhibitors (SSRIs), which are believed to be the first line of therapy for depression and anxiety disorders [22]. Our work fills in a significant vacuum in the literature despite the amount of information available on *A. galanga* extracts since, despite this plant's well-known traditional medicinal uses, not much scientific research has been done on it. The comprehensive chemical analysis using Gas chromatography-mass spectrometry (GC-MS) is a pioneering approach, revealing a unique and rich chemical composition. GC-MS comprehensive chemical analysis is an innovative method that reveals a distinct and complex chemical makeup. This research provides strong evidence of the extract's strong antioxidant, anticancer, and antibacterial properties in addition to quantifying the levels of total phenolic content (TPC) and total flavonoid content (TFC). These results provide fresh insights into the possible medicinal uses of *A. galanga*, particularly concerning the extract's ability to induce apoptosis in cancer cell lines and its powerful antibacterial activity against different strains. Therefore, the primary objectives of the current study were four-fold: i) To examine the *in vitro* antitumor role of *A. galanga* against breast cancer (MCF-7) and hepatocellular carcinoma (HepG2) cells and elucidate the underlying mechanism using the 3-[4,5-dimethylthiazol-2-yl]-2,5 diphenyl tetrazolium bromide (MTT) proliferation test and quantitative reverse transcription polymerase chain reaction(RT-qPCR) based mRNA expression profile of selected pro- and anti-apoptosis marker genes; ii) To evaluate the phytochemical composition and antioxidant properties of *A. galanga* rhizome extract (AgRE) via DPPH and ABTS assays, iii) To assess the antibacterial activity of AgRE against Gram-positive and Gram-negative bacteria using the MIC and minimum bactericidal concentration (MBC) methods; and iv) To apply molecular docking (MD) to assess the binding affinity of the most enriched constituents in AgRE toward the active sites of NADPH oxidase and p53 tumor suppressor protein (TP53).

## 2. Materials and methods

### 2.1. AgRE preparation

The rhizome of *A. galanga* was obtained from a local market in Riyadh, Saudi Arabia. The plant species was authenticated by Professor Dr. Mohammed Fasil from the Department of Botany and Microbiology, College of Science, King Saud University, Riyadh, Saudi Arabia. The extraction of *A. galanga* was prepared by extraction with methanol as described previously by Ref. [23]. In brief, the sample was ground into a powder after being rinsed under running water and dehydrated in the shade for one week and three days at 25 °C. Five grams of *A. galanga* powder was extracted by dissolving it in 50 ml of methanol: water (80:20, v/v) with stirring for 3 h. A mixture of methanol and water allows for the separation of polar components from non-polar components [24]. The extract was fitted through filter paper, and centrifugation and evaporation were performed with a rotary. The resulting extract was kept at 4 °C for further analysis.

### 2.2. Identification of compounds

AgRE was analyzed on a GC-MS system coupled to an Agilent 5977A MSD system (Agilent Technologies Inc., Santa Clara, CA, USA). A 30-m-long capillary column with a diameter of 0.25 mm and a film thickness of 0.25 μm was used to purify the volatile components found in the methanol extract. Helium was used as the carrier gas, and it flowed through the column at a steady rate of 1 ml per minute. At 250 °C, the injector temperature was kept constant. With a split ratio of 50:1, the injection volume in split mode was 1 L. The following temperature was selected for the oven: After 3 min, the oven's temperature was raised to 70 °C. It was then raised to 100 °C at a pace of 3 °C/min. It was then raised to 120 °C at a rate of 10 °C/min. It was then raised to 220 °C at a rate of 10 °C/min. An EI source, 70 eV electron energy, 230 °C ionization temperature, 280 °C interface temperature, 150 °C MS quadrupole temperature, and a quantity scanning range of 20–500 amu were the MS parameters.2.3 Antioxidant activity.

### 2.3. Antioxidant activity

#### 2.3.1. Determination of total TPC

The TPC in AgRE was determined using a modification of the Folin–Ciocalteu method as described in Ref. [25]. A standard curve was created using gallic acid solutions (25–150 μg/ml). A combination of 1.5 ml of ultrapure (Milli-Q) water, 0.1 ml of plant extract (1 mg/ml) or gallic acid, and 0.1 ml of Folin–Ciocalteu reagent was allowed to settle for 8 min. A volume of 0.3 ml of 20 % sodium carbonate solution was added and mixed well using a vortex. The reaction mixture was left in the dark for 2 h. Using a UV–visible spectrophotometer, the absorbance of the resulting blue color was measured at 765 nm. The total phenols in AgRE content were expressed in milligrams of gallic acid equivalents (mg GAE/100 g extract).

#### 2.3.2. Determination of total TFC

The TFC in AgRE was determined using the method reported by Ref. [26]. A mixture of 1.0 ml of plant extract (1 mg/ml) and 1.0 ml of 2 % $AlCl_3$ water solution was prepared. The absorbance at 420 nm was measured after 1 h of incubation at room temperature. A standard curve ($R^2 = 0.9996$) was generated using a quercetin (QE) solution (50–800 μg/ml). The total flavonoid content of AgRE was calculated as equivalents in mg QE/100 g extract).

#### 2.3.3. DPPH assay

The radical scavenging action of *A. galanga* rhizome on DPPH was tested using the method developed by Ref. [27]. In brief, the DPPH solution (2 ml, 0.08 mM) was blended with the sample solution (2 ml) and then stored at room temperature in the dark for 30 min. The optical density was measured at 517 nm. Positive controls were ascorbic acid and BHT. The data were given as half-maximal inhibitory concentration ($IC_{50}$) values, and the control solutions and % of DPPH were analyzed using the following equation: DPPH radical scavenging activity [%] = $[(Ac - As)/Ac] \times 100$, where *Ac* denotes the absorbance of the control, and *As* denotes the absorbance of the sample.

#### 2.3.4. ABTS assay

ABTS was performed using the method described by Ref. [19]. ABTS solution (192 mg in distilled water to 50 ml) was mixed with $K_2S_2O_8$ solution (140 mM). After that, the mixture was stored at room temperature in the dark for 12 h. After mixing the ABTS solution with methanol, the $OD_{734}$ was adjusted from 0.02 to 0.70. Fifty microliters of each concentration were mixed into 3 ml of diluted ABTS. The OD was directly measured at 734 nm after a 6-min incubation period in the dark at room temperature. Positive controls were ABHT and ascorbic acid. The findings were provided as a percentage of the DPPH and $IC_{50}$ values.

### 2.4. Cell culture and cytotoxicity assays

In this work, human hepatoma HepG2 (ATCC HB-8065) and breast cancer MCF-7 (ATCC HTB-22) cell lines were employed as functioning *in vitro* model systems to investigate the lethal characteristics of several plant extracts [28,29]. The cells were cultured at 37 °C in a 5 % CO2 humidified environment using Dulbecco's Modified Eagle Medium (DMEM), supplemented with 1 % penicillin-streptomycin and fetal calf serum (FCS). Utilizing the 3-(4,5-dimethyl-2-thiazolyl)-2,5-diphenyl-2H tetrazolium bromide

(MTT) test, AgRE's cytotoxicity towards MCF-7 and HepG2 cells was evaluated. The MTT processing was carried out following the guidelines provided in our current study [30], and the $IC_{50}$ was calculated using the Graph Pad Prism program.

### 2.5. RT-PCR assay of apoptosis genes

Apoptotic (*caspase-3*, *8*, *9*, and *Bax*) and anti-apoptotic (*Bcl-xL* and *Bcl-2*) genes were identified using RT-PCR. Two thousand MCF-7 and HepG2 cells were gathered and arranged in six-well plates with 3 ml of growth medium combined with 400 μg/ml of AgRE. Morphological alterations in MCF-7 and HepG2 cells were evaluated using an inverted microscope (Eclipse TS100, Nikon, Japan). The supernatant was collected and the pellet was utilized for RNA using an RNeasy kit (Qiagen, Hilden, Germany) after centrifugation at 500*g* for 5 min at 4 °C. The RT-PCR used this RNA as a template. We followed the protocol for RT-qPCR as it was presented in our recent work [30].

### 2.6. Antibacterial activity

#### 2.6.1. Collection of microbial strains

*2.6.1.1. Disc diffusion assay.* The antibacterial activity of AgRE was evaluated by the agar well diffusion method as previously mentioned, [31]. The test was performed against six bacteria, three Gram-positive (*Staphylococcus aureus* (MTCC) −29213; *Staphylococcus epidermidis,* MTCC-12228; *B. subtilis*, MTCC-10400) and three Gram-negative (*E. coli*, ATCC-25922; *Pseudomonas aeruginosa*, MTCC-27853; *Klebsiella pneumonia*, MTCC-13883). On Muller Hinton Agar (MHA), six bacteria were subcultured in 100 μL ($1.0 \times 10^7$ bacterial CFU/ml). Using a sterile cork-borer, boreholes with a 5 mm diameter were punched at equal intervals on the surface to form wells. Petting the different concentrations of AgRE (100, 200, 400, and 800 μg/ml; 100 μL/well) into the wells was the next step. Muller Hinton Broth (HMB) with 0.1 % DMSO served as the negative control, while chloramphenicol (25 μg/ml) served as the positive control. The Petri dishes were incubated at 37 °C for 24 h to facilitate microbial development and evaluate the zone of inhibition around every AgRE-containing well.

#### 2.6.2. Determination of MIC and MBC

The MIC and MBC were measured using the microdilution method according to according to Ref. [32] using the 2,3,5-triphenyl tetrazolium chloride (TTC) method, as described by Ref. [32], with some changes. First, a primary culture of pathogenic bacteria was prepared at a concentration of $5 \times 10^6$ CFU/ml. Next, the extract (i.e., 1.95–1000 μg/ml)) was diluted with MHB. A 96-well plate was filled with 100 μL of the extract and bacteria were added to each well. At 37 °C, the plate was incubated for 24 h. Following the addition of TTC (20 μL; 2 mg/mL) to each well, the development of a reddish hue, indicating the proliferation of microorganisms, was monitored. The MIC was defined as the concentration at which no color shift was seen. Each well's contents (100 μL) that showed no color change were cultured on MHA and incubated for 24 h at 37 °C. MBC was a minimal dilution that prevented growth [33].

### 2.7. In silico analysis

#### 2.7.1. Ligand preparation

All chemical compositions identified in AgRE by GC-MS were downloaded from the PubChem database in SDF format. The ligands intended for docking were generated through the application of the OPLS3 force field, carried out within the LigPrep module of Maestro by Schrödinger. A maximum of 32 varieties of structural forms were derived from each initial input structure, encompassing alterations in stereochemistry, ionization, and tautomeric configurations. These structures then underwent processes involving energy minimization and geometric optimization. The establishment of ionization and tautomeric conditions occurred at a physiological pH of $7.0 \pm 2.0$, a process executed using Epik [34]. Currently, most drugs used in therapeutic settings work by inhibiting or activating enzymes to produce their pharmacological effects. To ascertain the binding interactions on the active site of the PON1 enzyme, a prior investigation based on MD studies of several medicines, including pemetrexed disodium, irinotecan hydrochloride, dacarbazine, and azacytidine, was conducted. PON1 was shown to be substantially inhibited by these drugs, with Ki constants ranging from $8.29 \pm 1.47$ μM to $23.34 \pm 2.71$ mM [20].

#### 2.7.2. Receptor preparation

For the docking investigation in this work, we selected two proteins, such as P53 and NADPH oxidase. NADPH oxidase, a key enzyme found in various cells including immune cells and endothelial cells, plays a crucial role in antioxidant activity through its generation of reactive oxygen species (ROS). While traditionally known for its role in the immune response, NADPH oxidase also contributes to redox signaling and maintenance of cellular homeostasis. Inhibiting NADPH oxidase activity holds significant promise in enhancing antioxidant activity and mitigating oxidative stress-related damage. By blocking the enzymatic function of NADPH oxidase, the production of ROS is attenuated, thereby reducing oxidative stress within cells and tissues. P53 is known as a guardian of the genome, organizing cellular responses to DNA damage, its inhibition has been explored as a potential strategy in certain contexts of cancer therapy. Inhibition of p53 can be advantageous in cancer cells harboring wild-type p53 that have become reliant on its activity for survival. By blocking p53 function, these cancer cells may become more susceptible to apoptosis. The structure of p53 (PDB ID: 3ZME, resolution: 1.35 Å) [35,36] and the crystal structure of NADPH oxidase (PDB ID: 2CDU, resolution: 1.80 Å) [37] were obtained

from the protein data bank. Within Maestro, Schrödinger integrated the Protein Preparation Wizard to guarantee the chemical accuracy and optimization of the proteins, rendering them suitable for modeling computations. During this phase, bond orders were assigned, hydrogen atoms were introduced into the structure, disulfide bonds were formed, zero-order bonds on metals were adjusted, and water molecules beyond a distance of 5 Å from heteroatoms were removed [34]. For example, the human metalloenzyme carbonic anhydrase (hCAs) has been markedly suppressed by the five antiviral medications abacavir, emtricitabine, lamivudine, ribavirin, and ritonavir at micromolar dosages, according to *in vitro* and *silico* study [38].

Ionization predictions and tautomeric states were determined at pH 7.0 for heteroatom groups using the relevant settings. Prime was employed to supplement any side chains missing from the protein's crystal structure. Hydrogen bonds were incorporated to simulate a pH of 7.0, which was chosen to represent an ionization state suitable for both acidic and essential amino acid residues. However, the introduction of hydrogen atoms sometimes led to steric clashes among the residues. These clashes were alleviated through energy minimization, utilizing the OPLS3 force field until an RMSD value of 0.30 Å was achieved [39].

### 2.7.3. Receptor grid generation

The investigation and characterization of the active site (binding pockets) within the p53 and NADPH oxidase proteins were done using the Receptor Grid Generation wizard of the Maestro software selected on an atom in the original ligand (an option offered by the Receptor Grid Generation wizard). Only one active site was generated and used for the subsequent grid creation. The proton-pump inhibitors (PPIs) inhibited paraoxonase 1 activity at low doses, the binding scores reported *in silico* studies were found to correspond with the acquired from in-vitro experimental results [40].

For docking, the Receptor Grid Generation tool was employed to generate a grid box at the center of the active site. The grid coordinates of each protein were determined as follows.

| Protein | Grid box coordinates | | |
|---|---|---|---|
| | X | Y | Z |
| P53 | 91.626 | 94.276 | −44.869 |
| NADPH oxidase | 19.853 | −6.431 | −0.896 |

### 2.7.4. MD

The scoring process for ligands was conducted using the Glide module of the Schrödinger program with standard settings in Standard Precision mode, as described in Ref. [30]. Within this process, Glide employed a hierarchical sequence of filters to explore potential binding positions of the ligands within the receptor's active site. The ligands were treated as flexible entities, whereas the receptor was rigid except for the active site region. The resulting docking scores were computed, and the ligands were ranked based on their scores [34].

In a molecular modeling study, synthesized novel spiroindoline oxadiazolyl-based acetate derivatives were found to be effective in inhibiting the polyol pathway of several cardiovascular diseases, such as cardiomyopathy, myocardial ischemia, congestive heart failure, and cardiac hypertrophy. Additionally, these novel derivatives were found to be effective in preventing various complications related to Aldose reductase in diabetes, including retinopathy, nephropathy, and neuropathy [41].

## 2.8. Statistical analysis

Analysis of variance was performed on all gathered data. Each experiment was carried out three times independently, with the

**Table 1**
Volatile components in AgRE identified by GC-MS.

| | Compound | RT | Area | Area % | Molecular formula | Molecular weight g/mol | m/z ratio |
|---|---|---|---|---|---|---|---|
| 1 | 2,3-Butanediol | 3.94 | 1591278 | 1.570 | $C_4H_{10}O_2$ | 90.12 | 90.12 |
| 2 | 2-Methoxy-phenol | 8.64 | 1508832 | 1.490 | $C_7H_8O_2$ | 124.14 | 124.14 |
| 3 | 2-Methoxy-4-vinyl phenol | 12.02 | 176165 | 1.740 | $C_9H_{10}O_2$ | 150.17 | 150.17 |
| 4 | Curcumene | 14.60 | 1137219 | 1.120 | $C_{15}H_{22}$ | 202.33 | 202.33 |
| 5 | *β*-sesquiphellandrene | 15.23 | 739671 | 0.730 | $C_{15}H_{24}$ | 204.35 | 204.35 |
| 6 | Cymene | 16.02 | 2038420 | 2.020 | $C_{10}H_{14}$ | 134.22 | 134.22 |
| 7 | 1-Ethyl-4-(2-methylpropyl)-benzene | 16.63 | 684115 | 0.680 | $C_{12}H_{18}$ | 162.27 | 162.27 |
| 8 | 4,6,8-Tetradecatriene | 16.79 | 612257 | 0.610 | $C_{14}H_{16}O$ | 200.28 | 200.28 |
| 9 | *β*-turmerone | 17.20 | 59351332 | 58.710 | $C_{15}H_{22}O$ | 218.33 | 218.33 |
| 10 | 1-(1-Propynyl)-cyclohexene | 17.48 | 347251 | 0.340 | $C_9H_{12}$ | 120.19 | 120.19 |
| 11 | *α*-turmerone | 17.65 | 22765790 | 22.520 | $C_{15}H_{22}O$ | 218.33 | 218.33 |
| 12. | 4-(4-Hydroxy-3-3-buten-2-one | 19.00 | 1046495 | 1.040 | $C_8H_{16}O_3$ | 160.21 | 160.21 |
| 13 | 4-(4-Hydroxy-3-methoxy phenyl)-3-buten-2-one | 19.74 | 1077332 | 1.070 | $C_{11}H_{12}O_3$ | 192.21 | 192.21 |
| 14 | 9-Octadecenoic acid | 20.50 | 342299 | 0.340 | $C_{18}H_{34}O_2$ | 282.55 | 282.55 |
| 15 | 3-Decen-5-one | 20.89 | 834495 | 0.830 | $C_{10}H_{18}O$ | 154.25 | 154.25 |
| 16 | Z-8-methyl-9-tetradecenoic acid | 22.24 | 1191410 | 1.180 | $C_{15}H_{28}O_2$ | 240.38 | 240.38 |

results provided as the mean ± standard deviation (SD). Student's *t*-test was used to compare group differences. To compare groups, the Mann–Whitney *U* test was used for non-Gaussian variables. Results with $p < 0.05$ were determined to be significant.

## 3. Results

### 3.1. Chemical composition of AgRE

GC-MS analysis of the AgRE was performed in comparison to the mass spectra of the components using the National Institute of Standards and Technology (NIST) library. Mass spectrometry produces results for the mass-to-charge ($m/z$, where m is the mass and z is the charge ratio of ions in a compound [42]. As can be shown in Table 1 and Fig. 1, the AgRE included 16 distinct chemicals. $\beta$-turmerone (58.710 %), ($m/z = 218.33$) was the most abundant component of AgRE, followed by $\alpha$-turmerone (22.52 %), ($m/z = 218.33$) and cymene (2.02 %) ($m/z = 134.22$).

### 3.2. Antioxidant activity

#### 3.2.1. TPC and TFC

According to the correlation coefficient ($R^2 = 0.978$), the TPC in AgRE was 233.79 ± 2.18 (GAE)/g, whereas the number of TFC ($R^2 = 0.999$) was 143.13 ± 2.44 (QE)/g.

#### 3.2.2. Radical scavenging activity of DPPH and ABTS

DPPH and ABTS were used to assess the antioxidant activity of AgRE. AgRE had a moderate scavenging ability for DPPH and ABTS radicals with $IC_{50}$ values of 79.34 ± 1.78 and 88.94 ± 2.28 μg/ml, respectively (Fig. 2).

### 3.3. Anticancer activity

#### 3.3.1. Cytotoxic activity

The effect of AgRE on MCF-7 and HepG2 cells was examined for 24 h using the MTT test at various doses of AgRE (50–400 μg/ml). The results showed a substantial ($p < 0.05$) difference between untreated and treated cells at various doses (Fig. 3). At 100 μg/ml and above, AgRE significantly inhibited the growth of MCF-7 and HepG2 cells ($p < 0.05$); further concentrations of AgRE exerted gradient cytotoxic activity with increasing concentration; viability began to drop significantly ($p < 0.05$) at 200 and 400 μg/ml. Furthermore, AgRE showed higher potential anticancer activity and cytotoxicity in HepG2 cells than in MCF-7 cells, with $IC_{50}$ values of 125.35 ± 4.28 and 182.49 ± 3.19 μg/ml, respectively.

#### 3.3.2. Effects of AgRE on MCF-7- and HepG2-induced apoptosis signaling

RT-qPCR was used to assess the effect of AgRE on triggered apoptotic signaling in MCF-7 and HepG2 cells after 48 h. As illustrated in Fig. 4A, AgRE-treated MCF-7, and HepG2 cells had significantly higher caspase-3, -8, and -9 mRNA levels than control untreated cells, whereas AgRE-treated cells had a significantly higher caspase-3, -8, and -9 expression than control untreated cells ($p < 0.05$). As

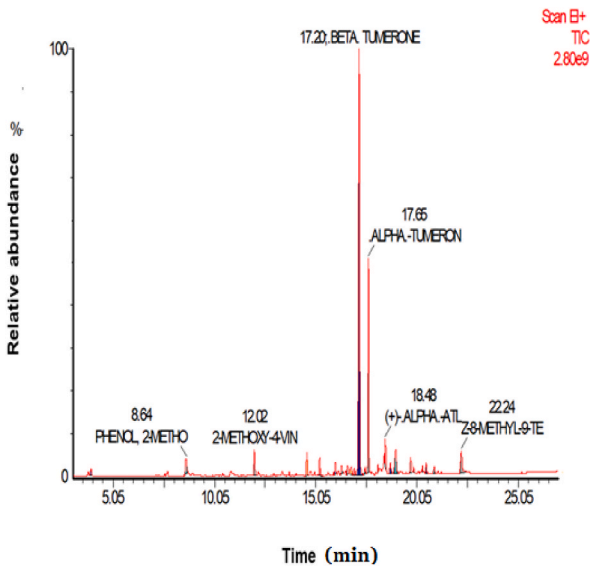


**Fig. 1.** The AgRE GC-MS chromatograms. For the investigation, methanol extract was used, and the GC–MS equipment was set for 73 min. Each identified peak in the spectrum indicates a known chemical, and the presence of a significant peak indicates the main component of the extract.

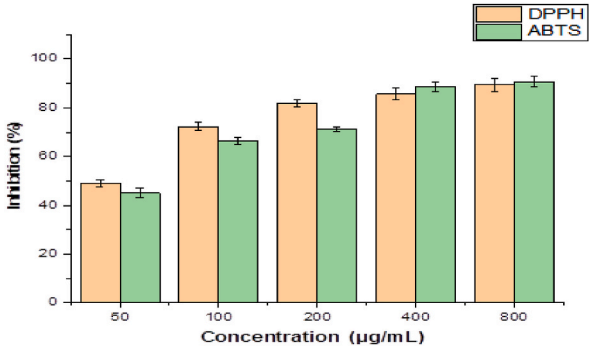


**Fig. 2.** Antioxidant activity of AgRE. The reported statistics are the mean and SD of three replicates.

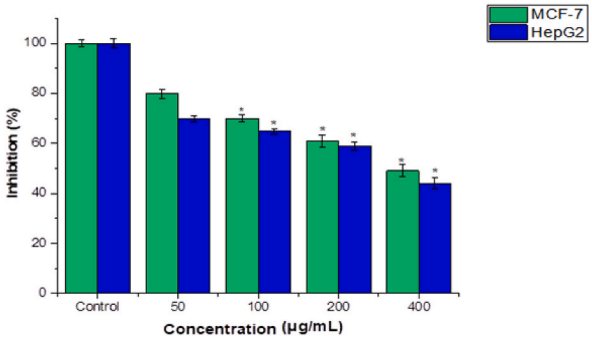


**Fig. 3.** The effect of AgRE on the viability of MCF-7 and HepG2 cells was determined using the MTT assay. The MTT assay was used to assess the cytotoxicity of AgRE on MCF-7 and HepG2 cells at doses ranging from 0 to 400 µg/ml for 24 h. The values represent the mean and SD of three independent experiments. * = a significant difference from the control (* = $p < 0.05$) is indicated.

shown in Fig. 4B, AgRE significantly elevated *Bax* mRNA and significantly reduced *Bcl-2* and *Bcl-xL* anti-apoptotic genes in treated MCF-7 and HepG2 cells compared to control untreated cells ($p < 0.05$). AgRE-treated MCF-7 and HepG2 cells had higher levels of *p21* and *p53* mRNA than untreated control cells ($p < 0.05$) (Fig. 4C).

### 3.4. Cells morphemically change

To observe the AgRE changes in morphology on the MCF-7 and HepG2 cell lines. AgRE was added at a concentration of 400 µg/mL to MCF-7 and HepG2 cells, and the cells were then incubated for 48 h in a humid environment (37 °C, 5 % CO2, 95 % air). Observed in (Fig. 5), AgRE-treated cells showed morphological changes after the incubation time, starting with the rounding of the cells and progressing to the formation of tiny aggregates and progressive detachment (Fig. 5B and D).

### 3.5. Antibacterial activity of AgRE

Fig. 6 displays AgRE's antibacterial efficacy against certain bacterial strains. The details of the antimicrobial activity zone comparison with positive drug control are shown in Table 2. The evaluated AgRE inhibited bacterial growth to varying degrees, with MICs ranging from 7.81 ± 1.53 to 62.5 ± 3.28 µg/ml. *S. epidermidis* (MTCC 12228) was the most sensitive strain, with MIC of 7.81 ± 1.53 µg/ml and MBC of 15.62 ± 1.25 µg/ml. AgRE had weak antibacterial activities against *K. pneumonia* (MTCC 13883), with MIC values of 62.5 ± 3.28 µg/ml and MBC of 125 ± 5.29 µg/ml.

### 3.6. MD

We used *in silico* docking analysis to study the binding affinities of the major AgRE compounds with the amino acids found in the active sites of NADPH oxidase (PDB: 2CDU) and P53 (PDB: 3ZME). The results showed that 1-ethyl-4-(2-methylpropyl)-benzene exhibited NADPH oxidase inhibitory activity, with a Glide score of −6848 kcal/mol, followed by 2-methoxy-phenol, with a Glide score of −5111 kcal/mol (Table 3). Docking of 1-ethyl-4-(2-methylpropyl)-benzene in the active site of NADPH oxidase showed the formation of a single hydrogen bond with residue ILE160 and a Pi–Pi stacking bond with residue PHE 245. By contrast, 2-methoxy-phenol established a single hydrogen bond with residue VAL 214 (Fig. 7A, B, 8A, and 8B).

Moreover, the phytochemical compounds identified in AgRE had a high affinity for the active site of p53. 1-Ethyl-4-(2-

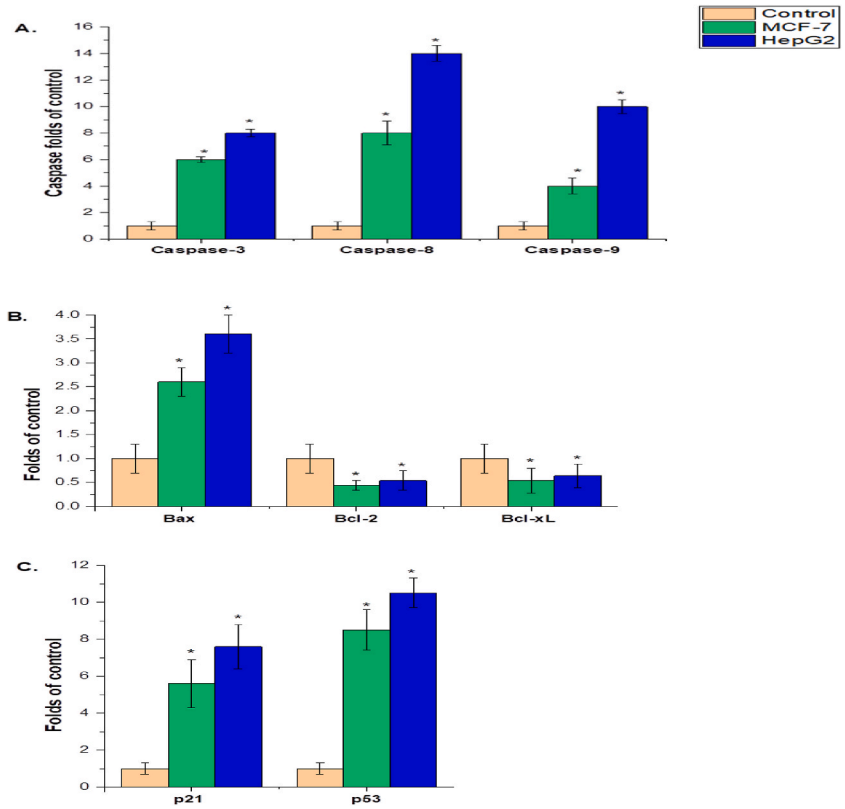


**Fig. 4.** Effect AgRE (400 μg/mL) on MCF-7 and HepG2 cell lines. AgRE significantly stimulate the activity of a percentage of the apoptotic population. **A:** *Caspase-3, 8*, and *9*. **B:** *Bax, Bcl-2*, and *Bcl-xL*. **C:** *p53* and *p21*. Values are mean ± SD. Gene expression was significantly (*) ($p < 0.05$) different from the negative control.

methylpropyl)-benzene was the most active molecule against the p53 active site, with a Glide score of −7497 kcal/mol, followed by cymene, with a Glide score of −6381 kcal/mol (Table 4, Fig. 7C, D, 8C, and 8D).

## 4. Discussion

Plant-derived chemicals are a major source of compounds for pharmaceuticals, which people have used for a variety of purposes for centuries [43]. In this line of research, drug discovery from secondary metabolites of medicinal plants led to the extraction of early medications such as ursolic acid, paclitaxel, camptothecin, podophyllotoxin, and combretastatin, all of which have anticancer, antioxidant, anti-inflammatory, and antibacterial properties [44,45]. We used GC-MS to analyze the chemical composition of AgRE in this work. In addition, we used the qPCR-based mRNA expression profile of selected pro- and anti-apoptosis marker genes to investigate the anticancer, antibacterial, and antioxidant capabilities, as well as possible apoptotic induction.

*A. galanga* (L.) is a significant rhizomatous plant that is used extensively as a flavorful culinary spice and in herbal remedies. The characteristics of *A. galanga* include being a perennial herb with a rhizome that is hard, cylindrical, and branched, with a strong aroma; an erect pseudostem; leaves that are lanceolate-oblong and alternate; an erect inflorescence that is terminal and has many fragrant, white or yellowish flowers; and globose to ellipsoidal capsules that range in color from yellow-orange to red [46]. According to our findings, AgRE contains a significant concentration of *α*-turmerone (58.710 %), followed by *β*-turmerone (22.52 %), and cymene (2.02 %). Turmerones (*α*-turmerone, *β*-turmerone, and ar-turmerone) are characteristic compounds that are the primary compounds in ginger family oil [47,48]. A prior study found that the essential oils from *A. galanga* flowers collected from subtropical (Pantnagar, India) and subtemperate (Purara, India) regions were dominated by β-pinene (12.8 and 10.5 %, respectively), 1,8-cineole (18.4 and 9.4 %, respectively), cis-sabinene hydrate (0 and 8.3 %, respectively), α-terpineol (4.5 and 3.4 %, respectively), and (E)-methyl cinnamate (19.7 and 7.1 %, resp.) for the two regions [49]. Additionally, the main volatile components of the *A. galanga* flowers (obtained from Yulin City, Guangxi Province, China) were found to be 64.3 % farnesene, followed by 3.6 % farnesyl acetate, 3.2 % aceteugenol, 3.1 % eugenol, 2.9 % E-nerolidol, 2.4 % decyl acetate, 2.0 % octyl acetate, 1.9 % sesquirosefuran, 1.7 % (E)-β-farnesene, and 1.5 % germacrene D [50]. Cineole (45.199 %), 4-allylphenyl acetate (13,718 %), α-farnesene (5.487 %), (2,6-dimethylphenyl) borate (5.023 %), and α-pinene (5.023 %) were among the major elements of *A. galangal* [21]. On the other hand, the two main phytochemical components identified in *A. galanga* leaf extracts were 3-phenyl-2-butanone (20.49 ± 0.6 %) and benzenepropanal (37.35 ± 0.5 %) [51]. Several studies have indicated that turmerones have pharmacological and therapeutic potential in a variety of biological

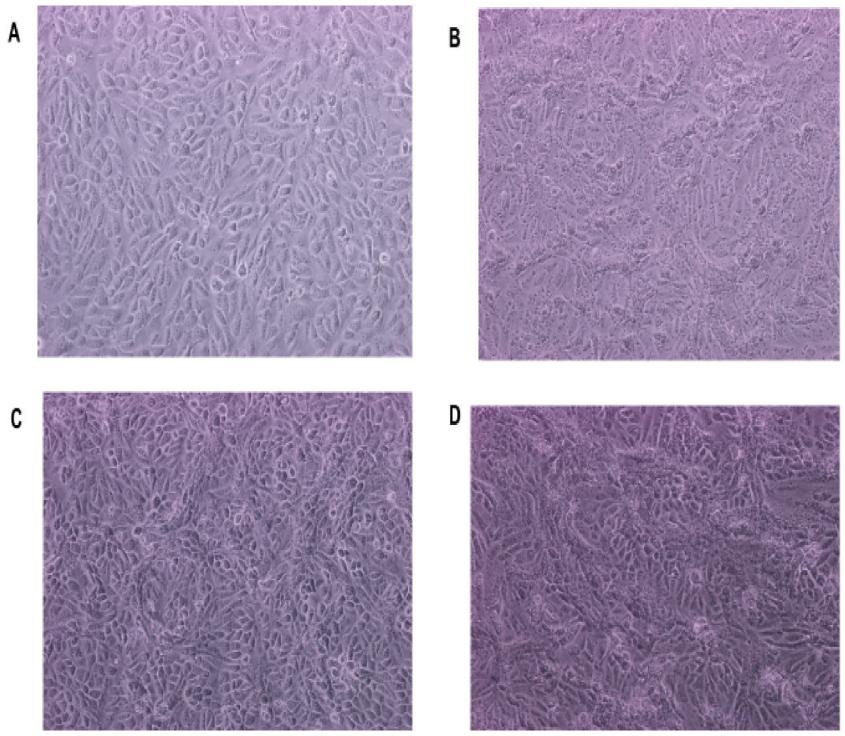


**Fig. 5.** Effect AgRE (400 μg/mL) on the HepG2 and MCF-7 cells morphology, (**A**) represents HepG2 non-treated cells, (**B**) represents HepG2 -treated cells with the AgRE (**C**) represents MCF-7 non-treated cells, (**D**) represents MCF-7 -treated cells with the AgRE. (Magnification power 10X).

activities, including anti-inflammatory properties [52–54], antifungal activities [55], and anti-proliferative efficacy against various human cancer cell lines [56–58].

In this work, we identified that AgRE is a promising source of phenol and flavonoid compounds. We observed that AgRE has moderate DPPH and ABTS radical scavenging activities, with $IC_{50}$ values of 391.20 ± 1.28 and 414.94 ± 1.28 μg/ml, respectively. Our results are similar to a recent study that demonstrated *A. galanga* flower essential oil has moderate DPPH and ABTS radical scavenging effects, with $IC_{50}$ values of 138.62 ± 3.07 and 40.48 ± 0.49 μg/ml, respectively [50]. An earlier study found that the essential oil of *A. galanga* has higher antioxidant activity, with $IC_{50}$ values of 550 μg/ml, than *Hyptis suaveolens*, with $IC_{50}$ values of 3721 μg/ml [59]. Furthermore, products containing phenols and flavonoids have been shown to have a considerable ability to scavenge non-physiological radicals such as DPPH and ABTS [27,60].

Cancer is a common disease that reduces the lifespan of individuals. Since 1970, cancer chemoprevention has been proposed as a feasible technique for reducing cancer incidence and mortality [61]. Natural substances are useful in cancer therapy, particularly as chemopreventive agents [62]. Novel chemicals with anticancer properties are still being discovered [63]. The limitations of current cancer medications have motivated researchers in the field of anticancer pharmaceuticals to seek innovative strategies to improve cancer treatment. Scientists have been studying the anticancer benefits of natural chemicals for the past decade because they can be used for cancer prevention with no noticeable adverse effects [64–66]. The MTT Assay is the most popular technique for high throughput screening of a compound's anti-proliferative properties on cultivated cells [67,68]. It is a colorimetric assay used to quantify cytotoxicity, cell viability, and proliferation. The MTT test is based on how live cells transform MTT into formazan crystals. This technique is widely used to detect the *in vitro* cytotoxic effects of medicines on cell lines or primary patient cells since, for most cell types, total mitochondrial activity is correlated with the number of viable cells [68]. In this study, extracts of *A. galanga* rhizome showed significant cytotoxic action ($p < 0.05$) against HepG2 cells and MCF-7 cells, with $IC_{50}$ of 125.35 ± 4.28 and 182.49 ± 3.19 μg/ml, respectively. These findings are consistent with those of an earlier study, in which an ethanolic extract of *A. galanga* was tested against many breast cancer cell lines, including 4T1, MCF-7, and T47D. After 48 h, the $IC_{50}$ value in 4T1 cells was 135 μg/ml, whereas in MCF-7 and T47D cells, it was 400 μg/ml and 170 μg/ml after 72 h, respectively [69]. Another study showed that *A. galanga*, gallic acid, and simvastatin were more cytotoxic to the HepG2 cell line [52]. Furthermore, *A. galanga* essential oil displayed significant selective cytotoxicity on K562 cells ($IC_{50}$ = 41.55 ± 2.28 μg/ml) and reduced cytotoxicity on non-cancerous L929 cells ($IC_{50}$ = 120.54 ± 8.37 μg/ml) [50]. *A. galanga* rhizome crude extract was also found to be low in normal cells (fibroblast cell line, NIH-3T3 cells) [70]. It was shown that the ethanolic extract of *A. galanga* had a cytotoxic effect because it contained antioxidant polyphenols that inhibited cell proliferation by interrupting the cell cycle [6].

Cancer cells are capable of evading apoptosis [71]. The mechanisms causing anticancer activity can be broadly divided into six categories: disruption of the membrane, a restriction of signaling pathways, autophagy modification, transcription regulation, cell

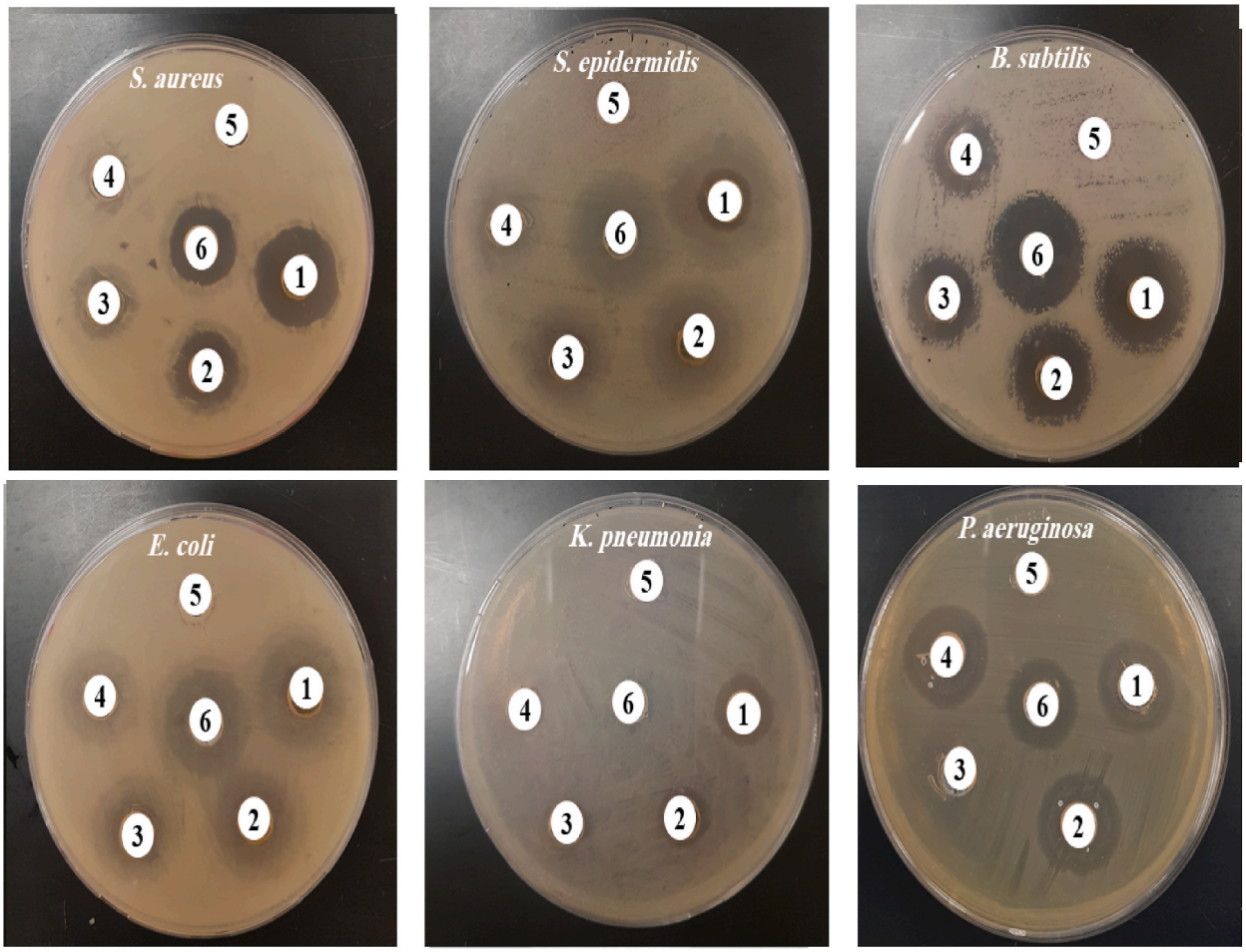


**Fig. 6.** Antibiogram demonstrating the antibacterial activity of AgRE against selected bacteria strains. (**1**) denotes 1000 μg/ml; (**2**) denotes 500 μg/ml; (**3**) denotes 250 μg/ml; (**4**) denotes 125 μg/ml; (**5**) denotes the negative control, 1 % DMSO with nutrient broth; (**6**) denotes the chloramphenicol-positive control.

**Table 2**
AgRE inhibitory zone (in mm), MIC, and MBC values against selected bacteria strains.

| Bacterium/Dilution | Positive control | 1000 μg/ml | 500 μg/ml | 250 μg/ml | 125 μg/ml | MIC (μg/ml) | MBC (μg/ml) |
|---|---|---|---|---|---|---|---|
| *S. aureus* (MTCC 29213) | 15 | 22 | 20 | 14 | 9 | 15.62 ± 1.25 | 31.25 ± 2.93 |
| *S. epidermidis* (MTCC 12228) | 26 | 32 | 26 | 19 | 15 | 7.81 ± 1.53 | 15.62 ± 1.25 |
| *B. subtilis* (MTCC 10400) | 24 | 21 | 19 | 15 | 12 | 15.62 ± 1.32 | 31.25 ± 1.17 |
| *E. coli* (ATCC 25922) | 25 | 22 | 20 | 15 | 13 | 31.25 ± 1.38 | 62.5 ± 1.77 |
| *K. pneumonia* (MTCC 13883) | 12 | 17 | 14 | 7 | 6 | 62.5 ± 3.28 | 125 ± 5.29 |
| *P. aeruginosa* (MTCC 27853) | 18 | 25 | 20 | 18 | 17 | 15.62 ± 2.33 | 31.25 ± 2.11 |

cycle arrest, and suppression of metabolic enzymes. For many anticancer therapy techniques, the gold standard has been to induce apoptosis in cancer cells. The majority of phytochemicals with anticancer effects cause target cells to undergo apoptosis. Apoptosis is a morphological process that is characterized by DNA fragmentation and cell shrinkage. It is controlled by a sequence of molecular processes that can be either intrinsically or extrinsically caused. The process of apoptosis has been primarily described concerning the activation of caspases, or cystine-aspartic proteases, as process effectors [6]. For example, AgRE increased apoptotic signaling in MCF-7 and HepG2 cells as demonstrated by a significant rise in caspase-3, -8, and -9 mRNA levels compared to untreated control cells ($p < 0.05$). An early *in vivo* study found that 1′-acetoxychavicol acetate in *A. galanga* had pro-apoptotic and anticancer effects by increasing caspase-8 and -9 activity and causing cycle cell arrest at GO/GI phase at a dose of 225 mg/kg BW/day for 2 weeks in breast, liver, kidney, and gastric cancer tissue from C3H mice [72]. Apoptosis is a kind of genetically controlled cell death that leads to the development of specific morphological features such as membrane blebbing and the production of apoptosis bodies [73]. Thus, apoptosis is emerging as a possible target for cancer therapy [74]. Three basic processes lead to apoptosis: intrinsic

**Table 3**
MD of ligands in the active sites of NADPH oxidase (PDB: 2CDU) and P53 (PDB: 3ZME).

| | Glide gscore (kcal/mol) | |
|---|---|---|
| | NADPH oxidase (PDB: 2CDU) | P53 (PDB: 3ZME) |
| 1-(1-Propynyl)-cyclohexene | −4.722 | −5.999 |
| 1-Ethyl-4-(2-methylpropyl)-benzene | −6.848 | −7.497 |
| 2,3-Butanediol | −2.913 | −4.03 |
| 2-Methoxy-4-vinylphenol | −4.783 | −5.706 |
| 2-Methoxy-phenol | −5.111 | −5.843 |
| 3-Decen-5-One | −2.71 | −3.925 |
| 4-(4-Hydroxy-3-methoxy phenyl)-3-buten-2-one | −3.583 | −5.108 |
| 4,6,8-Tetradecatriene | −5.08 | −5.316 |
| 9-Octadecenoic acid | −0.584 | −1.304 |
| $\alpha$-turmerone | −4.395 | −6.05 |
| $\beta$-sesquiphellandrene | −3.22 | −5.432 |
| $\beta$-turmerone | −4.543 | −6.138 |
| Curcumene | −3.965 | −5.895 |
| Cymene | −4.927 | −6.381 |
| Z-8-methyl-9-tetradecenoic acid | −2.652 | −2.318 |

(mitochondrial-mediated), extrinsic (death receptor-mediated), and endoplasmic reticulum stress-dependent signaling transduction. Caspase-8 is an important extrinsic pathway mediator; when activated, caspase-8 induces apoptosis by activating the executioner caspase-3, -6, and -7. Caspase-9 is a key upstream mediator in the intrinsic pathway that triggers apoptosis by activating caspase-3 and -7 [75]. Caspase-3 was shown to have both exogenous and endogenous apoptotic properties through interactions with caspase-8 and -9 [76]. Furthermore, our qPCR results revealed that *A. galanga* flower extract dramatically lowered the mRNA levels of anti-apoptotic genes *Bcl-2* and *Bcl-xL*, while increasing the levels of apoptosis-promoting genes (*Bax*, *p53*, and *p21*). *Bcl2*, an anti-apoptotic gene, prevents apoptosis by maintaining the integrity of the mitochondrial membrane. The Bax/Bcl2 ratio, it turns out, influences apoptotic sensitivity [77]. By modulating the activity of Bcl-2 family members, activated p53 causes cell cycle arrest, thus allowing DNA repair and/or apoptosis [78].

Overall, AgRE had antiproliferative effects in MCF-7 and HepG2 cells in the current study and has been linked to the treatment of various cancers via a plausible mode of action. Furthermore, the current study's findings suggest that AgRE may have anticancer activity through activating caspase signaling and the apoptotic pathway.

The increasing magnitude of antimicrobial resistance has reduced clinical efficacy while increasing treatment costs and mortality. This has pushed the field of microbiology to explore other novel antimicrobial strategies [79]. However, with no new antibiotics being developed and rising resistance even to last-resort antibiotics, antimicrobials can encourage the development of novel antimicrobial drugs. The use of natural medicines as a supplement to or alternative to traditional antibiotics is an exciting area of study [80,81]. In this study, the potential antibacterial activity of AgRE was evaluated using disk diffusion, MIC, and MBC assays. We found that all of the bacteria tested were sensitive to the antibacterial activities of AgRE, with MIC values ranging from 7.81 ± 1.53 to 62.5 ± 3.28 μg/ml. Of all tested bacteria, *S. epidermidis* (MTCC 12228) was inhibited the most by AgRE, with MIC of 7.81 ± 1.53 μg/ml and MBC of 15.62 ± 1.25 μg/ml, whereas *K. pneumonia* (MTCC 13883) was inhibited only at high concentrations, with MIC of 62.5 ± 3.28 μg/ml and MBC of 125 ± 5.29 μg/ml. *A. galanga* flower essential oil has recently been found to have strong antibacterial activity against *S. aureus, B. subtilis*, *P. aeruginosa*, and *Proteus* and showed moderate antibacterial properties against *Enterococcus faecalis*, with MIC values ranging from 3.13 to 6.25 mg/ml [50]. The antibacterial mechanism of *A. galanga* rhizome essential oil on *Enterohemorrhagic E. coli O157:H7* (*EHEC O157*) was investigated, and the results showed that its potent antibacterial activity was due to increased passive permeability of the bacterial cell membrane, followed by crucial intracellular component efflux. Furthermore, the essential oil of *A. galanga* rhizomes affected the intracellular physiological metabolism of *EHEC* O157, including the suppression of P-type ATPase activity and the down-regulation of four virulence genes linked with EHEC infections [13]. Recent research used ethanol, methanol, ethyl acetate, and water as four solvents to examine the antibacterial activity of galangal rhizome extracts. against diarrhea-causing *E. coli* K88 in pigs. Findings showed that galangal extract with ethyl acetate had substantially larger inhibitory diameters against *E. coli* K88 in comparison to galangal extracted with water, ethanol, and methanol [82]. The major antibacterial mechanisms include changes in cell membrane permeability, suppression of bacterial metabolism, inhibition of bacterial cell wall formation, and suppression of the synthesis of nucleic acids and proteins [83]. The mechanism of antibacterial action of *A. galanga* essential oil was reported in a previous study, the most susceptible bacteria to *A. galanga* oil among the tested bacteria was *E. coli*. Within 10 min, the oil visibly altered *E. Coli* cells. This destruction is presumably attributed to *A. galanga* oil, which is prone to interact with lipopolysaccharide on the bacterial cell membrane. The interaction altered the structure of the cell membrane [84].

MD is a powerful and reliable computational method for predicting diverse binding affinities and formats, in addition to investigating the underlying processes of ligand binding among distinct molecules and protein targets. In drug discovery and natural product structural biology, MD is an effective method for determining the mechanism of binding and the potency of ligand-protein associations [34,35]. Our MD findings revealed high binding affinities of the major constituents found in AgRE toward the active sites of NADPH oxidase and TP53 (Table 4, Figs. 6 and 7). NADPH oxidase is an enzyme complex responsible for generating ROS, which can contribute to oxidative stress and cellular damage when produced excessively. Therefore, inhibition of NADPH oxidase can reduce the levels of ROS and subsequently promote antioxidant activity within the cell [85]. P53 is a tumor suppressor protein that has a

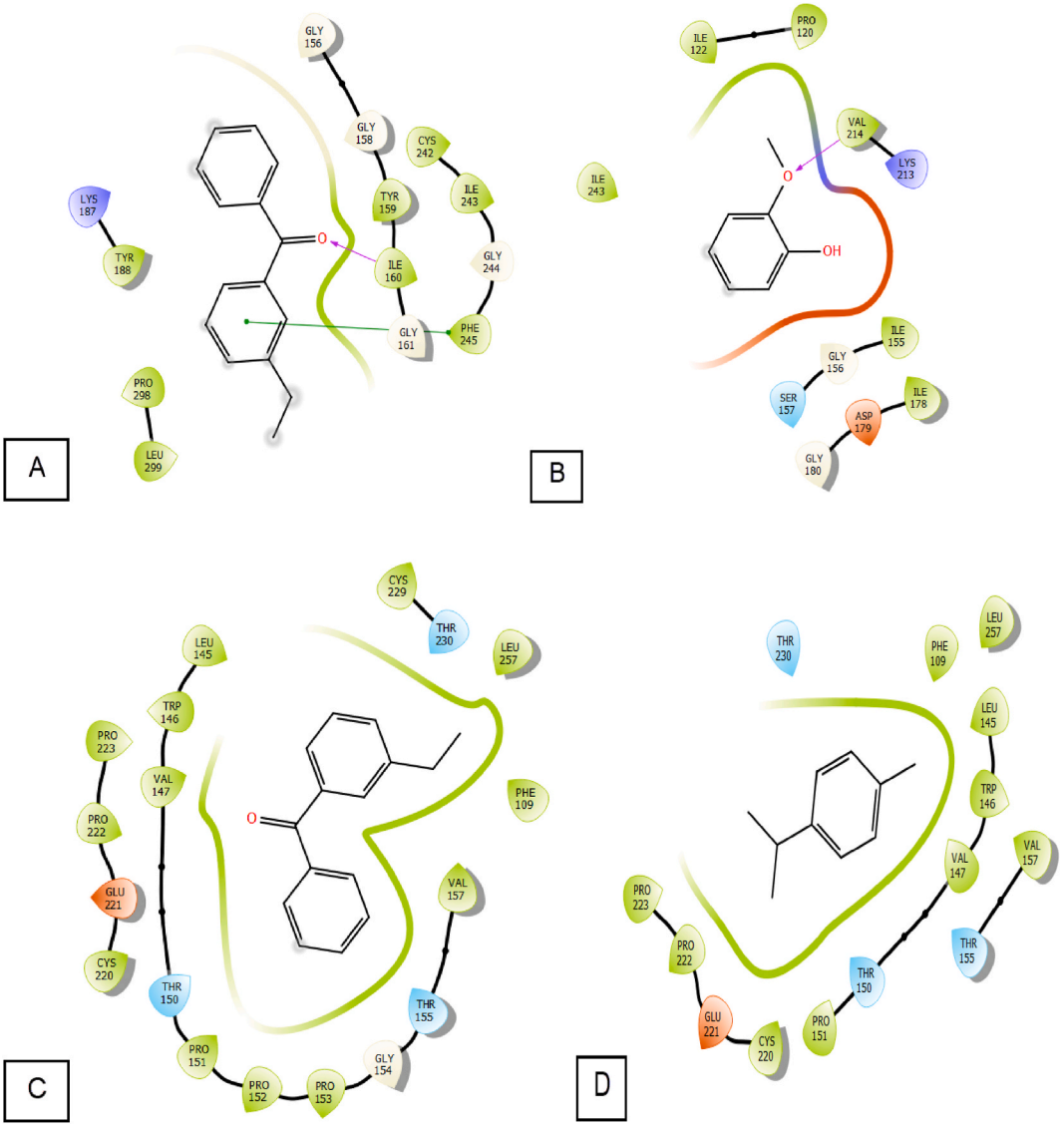


**Fig. 7.** Two-dimensional diagrams of ligand interactions with the active sites. **A and C:** 1-Ethyl-4-(2-methylpropyl)-benzene interactions with NADPH oxidase and P53 active sites. **B:** 2-Methoxy-phenol interactions with the NADPH oxidase active site. **D:** Cymene interactions with the P53 active site.

crucial role in regulating cell cycle progression, DNA repair, and apoptosis (programmed cell death). When p53 is inhibited, its ability to initiate appropriate responses to cellular stress, DNA damage, and other abnormalities is compromised, which can contribute to the development and progression of cancer. This inhibition can occur through various mechanisms, such as mutations in the *TP53* gene (which encodes the p53 protein), interactions with other proteins that disrupt its function, or changes in the cellular environment that affect its stability and activity. In the context of cancer treatment, inhibiting p53 may be a strategy to target cancer cells that have mutated p53 and rely on its dysregulated function for survival [86,87].

A limitation of this study was the lack of *in vivo* assays, which were not the primary focus. Therefore, additional *in vitro* and *in vivo* investigations are needed to study the supposed bioactivity of *A. galanga* against infectious diseases. AO/EB staining of MCF-7 and HepG2 cancer cell lines treated with AgRE and the hemolytic studies of AgRE were also required in future studies.

## 5. Conclusions

The GC-MS analysis showed that AgRE is an excellent source of $\beta$-turmerone and $\alpha$-turmerone. Like previous reports, the findings demonstrated that AgRE has powerful cytotoxic, antibacterial, and antioxidant properties, and minimizes the risk of developing complex diseases. In addition, AgRE preferentially promoted apoptosis in MCF-7 and HepG2 cells. As a result, *A. galanga* might be

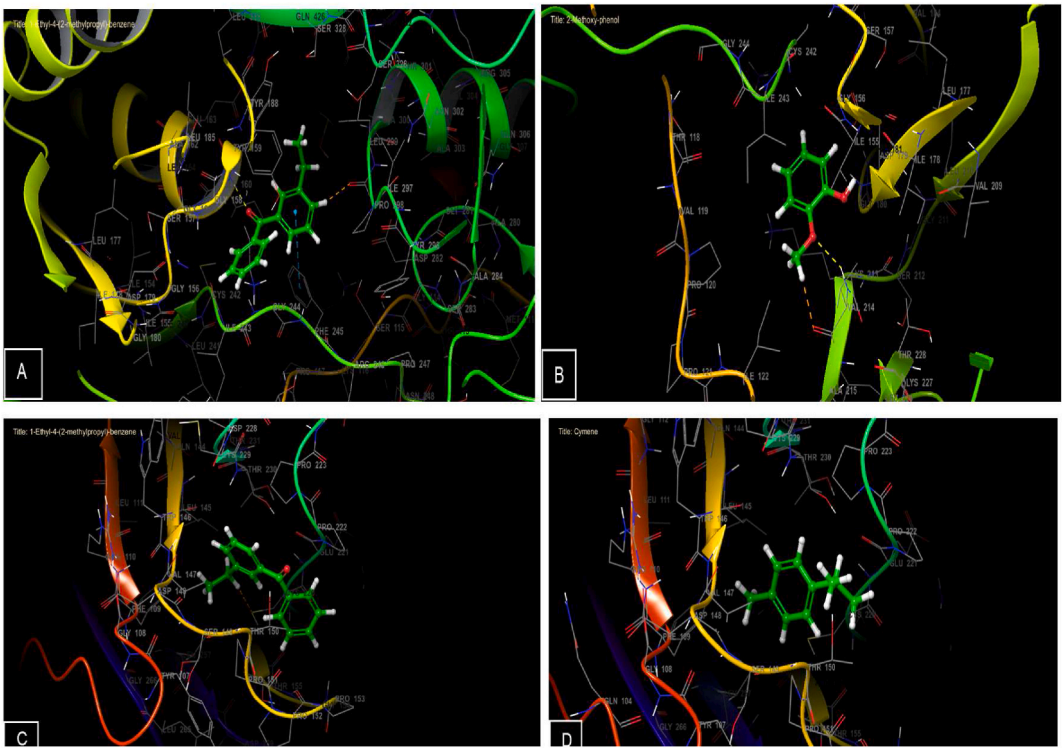


**Fig. 8.** Three-dimensional diagrams of ligand interactions with the active sites. **A** and **C:** 1-Ethyl-4-(2-methylpropyl)-benzene interactions with NADPH oxidase and P53 active sites. **B:** 2-Methoxy-phenol interactions with the NADPH oxidase active site. **D:** Cymene interactions with the P53 active site.

considered a bioactive natural product with significant potential in the pharmaceutical sector. Future research is necessary to understand the processes underlying AgRE's antioxidant and antibacterial properties. Further *in vitro* and *in vivo* research is also needed to investigate the alleged bioactivity of *A. galanga* against infectious illnesses and cancer.

## Ethics approval and consent to participate

The conducted research is not related to either human or animal use. However, the collection of plant materials was conducted following the guidelines of the International Union for Conservation of Nature (IUCN) policies research involving species at risk of extinction and the Convention on the Trade in Endangered Species of Wild Fauna and Flora. The cell lines were provided by the Virology Research Laboratory (VRG) group, College of Science, King Saud University, Saudi Arabia. All cell lines were maintained at 37 °C in and were mycoplasma-free (LookOut® Mycoplasma qPCR Detection Kitm, MERK).

## Data Availability

Data included in article/supp. materials/referenced in the article.

## CRediT authorship contribution statement

**Ibrahim M. Aziz:** Writing – original draft, Software, Methodology. **Akram A. Alfuraydi:** Validation, Software, Resources. **Omer M. Almarfadi:** Writing – review & editing, Data curation. **Mourad A.M. Aboul-Soud:** Writing – review & editing, Validation, Methodology. **Abdullah K. Alshememry:** Writing – review & editing. **Asma N. Alsaleh:** Writing – review & editing, Formal analysis. **Fahad N. Almajhdi:** Validation, Supervision.

## Declaration of competing interest

The authors declare that they have no known competing financial interests or personal relationships that could have appeared to influence the work reported in this paper.

## Acknowledgments

The authors thank the Researchers Supporting Project number (RSPD2024R536), King Saud University, Riyadh, Saudi Arabia.

## References

[1] A.N. Panche, A.D. Diwan, S.R. Chandra, Flavonoids: an overview, Journal of nutritional science 5 (2016) e47.
[2] J.E.W. Paz, C.R. Contreras, A.R. Munguía, C.N. Aguilar, M.L.C. Inungaray, Phenolic content and antibacterial activity of extracts of Hamelia patens obtained by different extraction methods, Braz. J. Microbiol. 49 (2018) 656–661.
[3] I. Bourais, S. Elmarrkechy, D. Taha, Y. Mourabit, A. Bouyahya, M. El Yadini, et al., A review on medicinal uses, nutritional value, and antimicrobial, antioxidant, anti-inflammatory, antidiabetic, and anticancer potential related to bioactive compounds of J. Regia, Food Rev. Int. (2022) 1–51.
[4] S. Hashem, T.A. Ali, S. Akhtar, S. Nisar, G. Sageena, S. Ali, et al., Targeting cancer signaling pathways by natural products: exploring promising anti-cancer agents, Biomed. Pharmacother. 150 (2022) 113054.
[5] K.A. Adedokun, S.O. Imodoye, I.O. Bello, A.-A. Lanihun, Therapeutic potentials of medicinal plants and significance of computational tools in anti-cancer drug discovery, in: Phytochemistry, Computational Tools and Databases in Drug Discovery, Elsevier, 2023, pp. 393–455.
[6] A. Suciati, Systematic review: anticancer potential of active compounds from galangal (Alpinia galanga), in: 4th International Conference Current Breakthrough in Pharmacy (ICB-Pharma 2022), Atlantis Press, 2022, pp. 269–282.
[7] T.K. Lim, Edible Medicinal and Non-medicinal Plants, Springer, 2012.
[8] C. Chen, C. Lin, C. Kao, H. Yeh, H. Li, C. Chang, Secondary metabolites from the rhizomes of Alpinia officinarum, Chem. Nat. Compd. 55 (2019) 1176–1178.
[9] A. Chudiwal, D. Jain, R. Somani, Alpinia galanga willd. An Overview on Phyto-Pharmacological Properties, 2010.
[10] T. Ai, Medicinal Flora of China, vol. 12, Peking University Medical Press, Beijing, China, 2016, pp. 330–332.
[11] S. Sahoo, S. Singh, A. Sahoo, B.C. Sahoo, S. Jena, B. Kar, et al., Molecular and phytochemical stability of long term micropropagated greater galanga (Alpinia galanga) revealed suitable for industrial applications, Ind. Crops Prod. 148 (2020) 112274.
[12] Y. Ye, X. Zhou, J. Huang, Ex Situ Flora of China (Zingiberaceae), China Forestry Publishing House, Beijing, China, 2020.
[13] C. Zhou, C. Li, S. Siva, H. Cui, L. Lin, Chemical composition, antibacterial activity and study of the interaction mechanisms of the main compounds present in the Alpinia galanga rhizomes essential oil, Ind. Crop. Prod. 165 (2021) 113441.
[14] L. Zhang, X. Liang, Z. Ou, M. Ye, Y. Shi, Y. Chen, et al., Screening of chemical composition, anti-arthritis, antitumor and antioxidant capacities of essential oils from four Zingiberaceae herbs, Ind. Crops Prod. 149 (2020) 112342.
[15] A. Kilic, L. Beyazsakal, M. Işık, C. Türkeş, A. Necip, K. Takım, et al., Mannich reaction derived novel boron complexes with amine-bis (phenolate) ligands: synthesis, spectroscopy and in vitro/in silico biological studies, J. Organomet. Chem. 927 (2020) 121542.
[16] J.H. Lee, Exploring natural compounds for anticancer activity: a focus on saussurea costus, Cancer Lett. 497 (2022) 207–216.
[17] R. Gupta, Anticancer potential of medicinal plants and their compounds: an overview, Int. J. Cancer Res. 17 (2021) 42–56.
[18] M. Fridlender, Y. Kapulnik, H. Koltai, Plant derived substances with anti-cancer activity: from folklore to practice, Front. Plant Sci. 6 (2015) 799.
[19] A. Buza, C. Türkeş, M. Arslan, Y. Demir, B. Dincer, A.R. Nixha, et al., Discovery of novel benzenesulfonamides incorporating 1, 2, 3-triazole scaffold as carbonic anhydrase I, II, IX, and XII inhibitors, Int. J. Biol. Macromol. 239 (2023) 124232.
[20] C. Türkeş, Investigation of Potential Paraoxonase-I Inhibitors by Kinetic and Molecular Docking Studies: Chemotherapeutic Drugs, vol. 26, Protein and peptide letters, 2019, pp. 392–402.
[21] A. Hamad, A. Alifah, A. Permadi, D. Hartanti, Chemical constituents and antibacterial activities of crude extract and essential oils of Alpinia galanga and Zingiber officinale, Int. Food Res. J. 23 (2016) 837.
[22] F. Akbarzadeh, M. Eslamzadeh, G. Behravan, A. Ebrahimi, S.A. Emami, A. Gilan, et al., Assessing the effect of Alpinia galanga extract on the treatment of SSRI-induced erectile dysfunction: a randomized triple-blind clinical trial, Front. Psychiatr. 14 (2023) 1105828.
[23] S.E. Lee, H.J. Hwang, J.-S. Ha, H.-S. Jeong, J.H. Kim, Screening of medicinal plant extracts for antioxidant activity, Life Sci. 73 (2003) 167–179.
[24] B. Sultana, F. Anwar, M. Ashraf, Effect of extraction solvent/technique on the antioxidant activity of selected medicinal plant extracts, Molecules 14 (2009) 2167–2180.
[25] K.L. Wolfe, R.H. Liu, Apple peels as a value-added food ingredient, J. Agric. Food Chem. 51 (2003) 1676–1683.
[26] A. Ordonez, J. Gomez, M. Vattuone, Antioxidant activities of sechium edule (jacq.) swartz extracts, Food Chem. 97 (2006) 452–458.
[27] M. Tian, X. Wu, T. Lu, X. Zhao, F. Wei, G. Deng, et al., Phytochemical analysis, antioxidant, antibacterial, cytotoxic, and enzyme inhibitory activities of Hedychium flavum rhizome, Front. Pharmacol. 11 (2020) 572659.
[28] T. Mosmann, Rapid colorimetric assay for cellular growth and survival: application to proliferation and cytotoxicity assays, J. Immunol. Methods 65 (1983) 55–63.
[29] A.A. Alkhudhayri, R. Wahab, M.A. Siddiqui, J. Ahmad, Selenium nanoparticles induce cytotoxicity and apoptosis in human breast cancer (MCF-7) and liver (HEPG2) cell lines, Nanosci. Nanotechnol. Lett. 12 (2020) 324–330.
[30] A.A. Alfuraydi, I.M. Aziz, F.N. Almajhdi, Assessment of antioxidant, anticancer, and antibacterial activities of the rhizome of ginger (Zingiber officinale), J. King Saud Univ. Sci. 36 (2024) 103112.
[31] N. Salem, S. Kefi, O. Tabben, A. Ayed, S. Jallouli, N. Feres, et al., Variation in chemical composition of Eucalyptus globulus essential oil under phenological stages and evidence synergism with antimicrobial standards, Ind. Crops Prod. 124 (2018) 115–125.
[32] D.F. Basri, V. Sandra, Synergistic interaction of methanol extract from Canarium odontophyllum Miq. Leaf in combination with oxacillin against methicillin-resistant Staphylococcus aureus (MRSA) ATCC 33591, International Journal of Microbiology 2016 (2016).
[33] M.M. Aljeldah, M.T. Yassin, A.A.-F. Mostafa, M.A. Aboul-Soud, Synergistic antibacterial potential of greenly synthesized silver nanoparticles with fosfomycin against some nosocomial bacterial pathogens, Infect. Drug Resist. (2022) 125–142.
[34] M.A. Aboul-Soud, H. Ennaji, A. Kumar, M.A. Alfhili, A. Bari, M. Ahamed, et al., Antioxidant, anti-proliferative activity and chemical fingerprinting of centaurea calcitrapa against breast cancer cells and molecular docking of caspase-3, Antioxidants 11 (2022) 1514.
[35] N. Kumar, P. Attri, D.K. Yadav, J. Choi, E.H. Choi, H.S. Uhm, Induced apoptosis in melanocytes cancer cell and oxidation in biomolecules through deuterium oxide generated from atmospheric pressure non-thermal plasma jet, Sci. Rep. 4 (2014) 7589.
[36] M. Abbasi, H. Sadeghi-Aliabadi, F. Hassanzadeh, M. Amanlou, Prediction of dual agents as an activator of mutant p53 and inhibitor of Hsp90 by docking, molecular dynamic simulation and virtual screening, J. Mol. Graph. Model. 61 (2015) 186–195.
[37] M. Bouslamti, A. Metouekel, T. Chelouati, A. El Moussaoui, A.E. Barnossi, M. Chebaibi, et al., Solanum elaeagnifolium var. Obtusifolium (dunal) dunal: antioxidant, antibacterial, and antifungal activities of polyphenol-rich extracts chemically characterized by use of in vitro and in silico approaches, Molecules 27 (2022) 8688.
[38] C. Türkeş, Carbonic anhydrase inhibition by antiviral drugs in vitro and in silico, J. Mol. Recogn. 36 (2023) e3063.
[39] F.E.-Z. Amrati, O.H.M. Elmadbouh, M. Chebaibi, B. Soufi, R. Conte, M. Slighoua, et al., Evaluation of the toxicity of Caralluma europaea (CE) extracts and their effects on apoptosis and chemoresistance in pancreatic cancer cells, J. Biomol. Struct. Dyn. (2022) 1–18.
[40] C. Türkeş, A potential risk factor for paraoxonase 1: in silico and in-vitro analysis of the biological activity of proton-pump inhibitors, J. Pharm. Pharmacol. 71 (2019) 1553–1564.
[41] Ö. Güleç, C. Türkeş, M. Arslan, Y. Demir, B. Dincer, A. Ece, et al., Novel spiroindoline derivatives targeting aldose reductase against diabetic complications: bioactivity, cytotoxicity, and molecular modeling studies, Bioorg. Chem. (2024) 107221.
[42] C. Wesdemiotis, K.N. Williams-Pavlantos, A.R. Keating, A.S. McGee, C. Bochenek, Mass spectrometry of polymers: a tutorial review, Mass Spectrom. Rev. 43 (2024) 427–476.

[43] E. Salmerón-Manzano, J.A. Garrido-Cardenas, F. Manzano-Agugliaro, Worldwide research trends on medicinal plants, Int. J. Environ. Res. Publ. Health 17 (2020) 3376.
[44] B. Réthy, B. Csupor-Löffler, I. Zupkó, Z. Hajdú, I. Máthé, J. Hohmann, et al., Antiproliferative activity of Hungarian Asteraceae species against human cancer cell lines. Part I, Phytother Res.: An International Journal Devoted to Pharmacological and Toxicological Evaluation of Natural Product Derivatives 21 (2007) 1200–1208.
[45] W. Ramakrishna, A. Kumari, N. Rahman, P. Mandave, Anticancer activities of plant secondary metabolites: rice callus suspension culture as a new paradigm, Rice Sci. 28 (2021) 13–30.
[46] T. Trimanto, L. Hapsari, D. Dwiyanti, Alpinia galanga (L.) willd: plant morphological characteristic, histochemical analysis and review on pharmacological, in: AIP Conference Proceedings, AIP Publishing, 2021.
[47] S. Li, W. Yuan, G. Deng, P. Wang, P. Yang, B. Aggarwal, Chemical composition and product quality control of turmeric, Curcuma longa, L.) 2 (2011) 28–54.
[48] Y. Takemoto, C. Kishi, H. Ehira, N. Matsui, T. Yamaguchi, Y. Yoshioka, et al., Inhaled turmerones can be incorporated in the organs via pathways different from oral administration and can affect weight-gain of mice, Sci. Rep. 12 (2022) 11039.
[49] R.C. Padalia, R.S. Verma, V. Sundaresan, C.S. Chanotiya, Chemical diversity in the genus Alpinia (Zingiberaceae): comparative composition of four Alpinia species grown in Northern India, Chem. Biodivers. 7 (2010) 2076–2087.
[50] Y. Tian, X. Jia, Q. Wang, T. Lu, G. Deng, M. Tian, et al., Antioxidant, antibacterial, enzyme inhibitory, and anticancer activities and chemical composition of Alpinia galanga flower essential oil, Pharmaceuticals 15 (2022) 1069.
[51] S. Singh, B.C. Sahoo, S.K. Kar, A. Sahoo, S. Nayak, B. Kar, et al., Chemical constituents analysis of Alpinia galanga and Alpinia calcarata, Res. J. Pharm. Technol. 13 (2020) 4735–4739.
[52] S.Y. Park, M.L. Jin, Y.H. Kim, Y. Kim, S.J. Lee, Anti-inflammatory effects of aromatic-turmerone through blocking of NF-κB, JNK, and p38 MAPK signaling pathways in amyloid β-stimulated microglia, Int. Immunopharm. 14 (2012) 13–20.
[53] S.Y. Park, Y.H. Kim, Y. Kim, S.-J. Lee, Aromatic-turmerone's anti-inflammatory effects in microglial cells are mediated by protein kinase A and heme oxygenase-1 signaling, Neurochem. Int. 61 (2012) 767–777.
[54] Y.-L. Li, Z.-Y. Du, P.-H. Li, L. Yan, W. Zhou, Y.-D. Tang, et al., Aromatic-turmerone ameliorates imiquimod-induced psoriasis-like inflammation of BALB/c mice, Int. Immunopharm. 64 (2018) 319–325.
[55] O.D. Dhingra, G.N. Jham, R.C. Barcelos, F.A. Mendonça, I. Ghiviriga, Isolation and identification of the principal fungitoxic component of turmeric essential oil, J. Essent. Oil Res. 19 (2007) 387–391.
[56] M. Ji, J. Choi, J. Lee, Y. Lee, Induction of apoptosis by ar-turmerone on various cell lines, Int. J. Mol. Med. 14 (2004) 253–256.
[57] G.G. Yue, B.C. Chan, P.-M. Hon, M.Y. Lee, K.-P. Fung, P.-C. Leung, et al., Evaluation of in vitro anti-proliferative and immunomodulatory activities of compounds isolated from Curcuma longa, Food Chem. Toxicol. 48 (2010) 2011–2020.
[58] S.-B. Cheng, L.-C. Wu, Y.-C. Hsieh, C.-H. Wu, Y.-J. Chan, L.-H. Chang, et al., Supercritical carbon dioxide extraction of aromatic turmerone from Curcuma longa Linn. induces apoptosis through reactive oxygen species-triggered intrinsic and extrinsic pathways in human hepatocellular carcinoma HepG2 cells, J. Agric. Food Chem. 60 (2012) 9620–9630.
[59] S. Tachakittirungrod, S. Chowwanapoonpohn, Comparison of antioxidant and antimicrobial activities of essential oils from Hyptis suaveolens and Alpinia galanga growing in Northern Thailand, J. Nat. Sci. 6 (2007) 31–42.
[60] L.K. Mailänder, P. Lorenz, H. Bitterling, F.C. Stintzing, R. Daniels, D.R. Kammerer, Phytochemical characterization of chamomile (matricaria recutita L.) roots and evaluation of their antioxidant and antibacterial potential, Molecules 27 (2022) 8508.
[61] S. Umezawa, T. Higurashi, Y. Komiya, J. Arimoto, N. Horita, T. Kaneko, et al., Chemoprevention of colorectal cancer: past, present, and future, Cancer Sci. 110 (2019) 3018–3026.
[62] C.-Z. Wang, Z. Zhang, S. Anderson, C.-S. Yuan, Natural products and chemotherapeutic agents on cancer: prevention vs. treatment, Am. J. Chin. Med. 42 (2014) 1555–1558.
[63] N.J. Jacobo-Herrera, F.E. Jacobo-Herrera, A. Zentella-Dehesa, A. Andrade-Cetto, M. Heinrich, C. Pérez-Plasencia, Medicinal plants used in Mexican traditional medicine for the treatment of colorectal cancer, J. Ethnopharmacol. 179 (2016) 391–402.
[64] M. Roepke, A. Diestel, K. Bajbouj, D. Walluscheck, P. Schonfeld, A. Roessner, et al., Lack of p53 augments thymoquinone-induced apoptosis and caspase activation in human osteosarcoma cells, Cancer Biol. Ther. 6 (2007) 160–169.
[65] M. Greenwell, P. Rahman, Medicinal plants: their use in anticancer treatment, Int. J. Pharmaceut. Sci. Res. 6 (2015) 4103.
[66] A.J. Siddiqui, S. Jahan, R. Singh, J. Saxena, S.A. Ashraf, A. Khan, et al., Plants in anticancer drug discovery: from molecular mechanism to chemoprevention, BioMed Res. Int. 2022 (2022).
[67] P. Wang, S.M. Henning, D. Heber, Limitations of MTT and MTS-based assays for measurement of antiproliferative activity of green tea polyphenols, PLoS One 5 (2010) e10202.
[68] Y. Rai, R. Pathak, N. Kumari, D.K. Sah, S. Pandey, N. Kalra, et al., Mitochondrial biogenesis and metabolic hyperactivation limits the application of MTT assay in the estimation of radiation induced growth inhibition, Sci. Rep. 8 (2018) 1531.
[69] S. Samarghandian, M.-A.-R. Hadjzadeh, J.T. Afshari, M. Hosseini, Antiproliferative activity and induction of apoptotic by ethanolic extract of Alpinia galanga rhizhome in human breast carcinoma cell line, BMC Compl. Alternative Med. 14 (2014) 1–9.
[70] F. Sandra, J. Sudiono, P. Trisfilha, D. Pratiwi, Cytotoxicity of Alpinia galanga rhizome crude extract on NIH-3T3 cells, The Indonesian Biomedical Journal 9 (2017) 23–28.
[71] A. Kornienko, Vr Mathieu, S.K. Rastogi, F. Lefranc, R. Kiss, Therapeutic agents triggering nonapoptotic cancer cell death, J. Med. Chem. 56 (2013) 4823–4839.
[72] Karlowee V, Tjahjono T, Wijayahadi N. Pengaruh Ekstrak Lengkuas Merah (Alpinia Galanga) Dosis Bertingkat Terhadap Ekspresi Caspase 3 Dan Grading Kanker Payudara Mencit C3H. MEDIA MEDIKA INDONESIANA. vol. 44: 92-100.
[73] N.S. Erekat, Programmed cell death in cerebellar Purkinje neurons, J. Integr. Neurosci. 21 (2022) 30.
[74] M. Hassan, H. Watari, A. AbuAlmaaty, Y. Ohba, N. Sakuragi, Apoptosis and molecular targeting therapy in cancer, BioMed Res. Int. 2014 (2014).
[75] L. Lossi, The concept of intrinsic versus extrinsic apoptosis, Biochem. J. 479 (2022) 357–384.
[76] M. Jiang, L. Qi, L. Li, Y. Li, The caspase-3/GSDME signal pathway as a switch between apoptosis and pyroptosis in cancer, Cell death discovery 6 (2020) 112.
[77] K.L. O'Neill, K. Huang, J. Zhang, Y. Chen, X. Luo, Inactivation of prosurvival Bcl-2 proteins activates Bax/Bak through the outer mitochondrial membrane, Genes Dev. 30 (2016) 973–988.
[78] S. Pal, J. Verma, S. Mallick, S.K. Rastogi, A. Kumar, A.S. Ghosh, Absence of the glycosyltransferase WcaJ in Klebsiella pneumoniae ATCC13883 affects biofilm formation, increases polymyxin resistance and reduces murine macrophage activation, Microbiology 165 (2019) 891–904.
[79] X. Wang, B. Loh, F. Gordillo Altamirano, Y. Yu, X. Hua, S. Leptihn, Colistin-phage combinations decrease antibiotic resistance in Acinetobacter baumannii via changes in envelope architecture, Emerg. Microb. Infect. 10 (2021) 2205–2219.
[80] M.H.H. Roby, M.A. Sarhan, K.A.-H. Selim, K.I. Khalel, Antioxidant and antimicrobial activities of essential oil and extracts of fennel (Foeniculum vulgare L.) and chamomile (Matricaria chamomilla L.), Ind. Crops Prod. 44 (2013) 437–445.
[81] B. Faehnrich, C. Franz, P. Nemaz, H.-P. Kaul, Medicinal plants and their secondary metabolites—state of the art and trends in breeding, analytics and use in feed supplementation—with special focus on German chamomile, J. Appl. Bot. Food Qual. 94 (2021) 61–74.
[82] D. Boonkusol, S. Sawasdee, J. Detraksa, K. Duangsrikaew, P. Watcharabundit, Evaluation of anti-Escherichia coli K88 from diarrhea piglets and phytochemicals of galangal rhizome extracts, Trends in Sciences 21 (2024) 7112, 7112.
[83] Y. Yan, X. Li, C. Zhang, L. Lv, B. Gao, M. Li, Research progress on antibacterial activities and mechanisms of natural alkaloids: a review, Antibiotics 10 (2021) 318.
[84] W. Prakatthagomol, S. Klayraung, S. Okonogi, Bactericidal action of Alpinia galanga essential oil on food-borne bacteria, Drug Discoveries & Therapeutics 5 (2011) 84–89.

[85] T.J. Guzik, D.G. Harrison, Vascular NADPH oxidases as drug targets for novel antioxidant strategies, Drug Discov. Today 11 (2006) 524–533.
[86] P.W. Hinds, R.A. Weinberg, Tumor suppressor genes, Curr. Opin. Genet. Dev. 4 (1994) 135–141.
[87] A.E. Ashour, A.F. Ahmed, A. Kumar, K.M. Zoheir, M.A. Aboul-Soud, S.F. Ahmad, et al., Thymoquinone inhibits growth of human medulloblastoma cells by inducing oxidative stress and caspase-dependent apoptosis while suppressing NF-κB signaling and IL-8 expression, Mol. Cell. Biochem. 416 (2016) 141–155.